Domain formation characteristics during thermomagnetic recording for amorphous TbFe and TbFeCo alloy thin films

Soon Gwang Kim, Seh Kwang Lee, Jong Chul Park
Chang Jin Kim, Myung Ryul Lee

Division of Materials Science and Engineering
Korea Advanced Institute of Science and Technology
P.O.Box 131 , Cheongryang , Seoul , Korea

ABSTRACT Static recording tests were carried out on a series of amorphous TbFe and TbFeCo thin films of various composition under a constant laser irradiation condition . Examination of recorded domain configurations by using polarizing microscope led to the categorization of domain characteristics into 3 distinctly different types; i.e., type A : circular domains with smooth boundaries, the size not sensitive to variation of bias field, type B : domains of irregular shape at low bias, the size increasing and the boundaries getting smoother and more circular with increasing bias field and type C : not recordable. Critical factor which distinguishes among each types was found to be the relative magnitude of H_c and H_d of the film near T_c, regardless of constituent atomic species. Micromagnetical process of thermomagnetic recording cycle was analyzed schematically for each type .

1. Introduction

Magneto-Optical(MO) memory is now generally accepted as the most promising information storage technology toward nineties[1]. One of the most crucial requirement to be improved in present MO media is the signal quality. Improvement of the magneto optical effect of the ferrimagnetic rare earth- transition metal amorphous alloy thin film which is now regarded as the first and the only commercially practical recording media at present has been a major target of research to this end since the signal quality of the MO media is directly proportional to the Kerr rotation angle, θ_k. More specifically, however, the signal quality is directly determined not only by the MO contrast of the cylindrically recorded magnetic domain(bit) but also by the size, shape and micromagnetical configuration of the bit[2,3]. Dimensional and micromagnetical characteristics of the recorded as well as erased bit is governed by thermomagnetic response of the medium material to the combined effect of the laser irradiation condition and applied bias field.

We introduce here some peculiar aspect of bit recording characteristics observed in a series of TbFe and TbFeCo thin films and suggested possible accounts of the underlying mechanisms for the observed experimental results.

2. Experimental

TbFe thin films of approximately 100nm-thickness were deposited on slide glass substrates by DC-magnetron sputtering from a 6-inch diameter Fe composite target arrayed with Tb chips. The composition of the film was adjusted by varying the area ratio of Tb chips to the Fe target. On the other hand, TbFeCo films were deposited on glass substrates by 3-target cosputtering. In both cases, sputtering pressure of argon gas was kept at 1.2mTorr following the evacuation of sputtering chamber down to 8x 10^{-7} Torr. Temperature dependence of the saturation magnetization of the films was determined by the vibrating sample magnetometry and the temperature dependence of coercivity with the polar Kerr hysteresis loop tracer of maximum field strength 11.5 KOe. Squareness of the shape of the Kerr hysteresis loop was regarded as a measure of perpendicular magnetization normal to the film plane. Composition of the films was analyzed by ICP spectroscopy. Thermomagnetic recording on the films was carried out

이 발표 논문은 과기처 특정연구과제와 관련된 논문입니다.

using a diode laser of the wavelength 830 nm. The focused laser beam radius was 0.5 μm. Maximum power of the laser diode installed in a TAOHS (Olympus Optical Co.) was 10 mW when measured on the film. Domain was imaged on the TV monitor through polarizing microscope and SIT TV camera. The variation range of applied bias field strength was ±300 Oe. In this work the laser recording condition was fixed at 9 mW power on the film surface for 13 μsec pulse duration time for all films recorded.

3. Results

3-1. Temperature Profile

In the course of laser irradiation and subsequent cooling the thin film medium undergoes continual change in both spatial and temporal temperature distribution. Assuming a Gaussian intensity profile of laser beam the temperature profile of thin film can be calculated numerically using the finite element method[4]. Fig.1 shows radial temperature distribution of the film when the peak temperature reaches maximum value, 225°C, under the laser irradiation condition of 9mW-13μsec. The thermal constants employed in the calculation are listed in Table 1, in which it is clearly seen that the thermal response of TbFe and TbFeCo is essentially identical and independent of the composition.

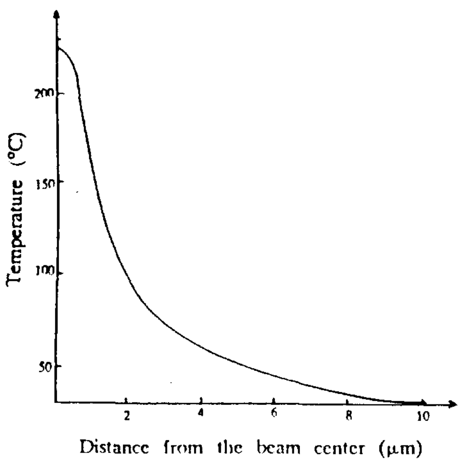

Fig.1 Radial temperature profile in thin film of 100nm thickness after laser irradiation of 9 mW - 13 μsec pulse duration.

3-2. Thermomagnetic Recording Characteristics of TbFe Films

Thermomagnetic recording experiments on a series of TbFe films with systematic variation of composition within the range exhibiting perpendicular magnetization revealed that the recording characteristics could be classified into 3

Table 1. Materials constants used for calculation

Material	Reflectivity	density× specific heat	thermal conductivity
$Tb_{20}Fe_{80}$	0.45	2.87	0.915
$Tb_{23}Fe_{77}$	0.45	2.78	0.925
TbFeCo	0.45	2.80	0.93
glass		1.81	0.0109
		(J/cc K)	(W/cm K)

different types according to the composition;
(1) compensation temperature(T_{comp}) <ambient temperature (T_a) : Type A, (2) $T_{comp}>T_a$: Type B and (3) $T_{comp} \leqq T_c$(Curie temperature) : Type C. However, since Type C films are essentially unrecordable due to steep rise of coercivity upon cooling down just below T_c, concern may be focussed on Type A and B only. Fig.2 shows typical domain characteristics of Type A (a-1) and B (a-2) recorded at a variety of external bias fields. Composition of the film shown here in Fig. 2 (a-1) and (a-2) is 20 and 23 at.% Tb, respectively. Since the compensation composition of TbFe alloy is about 22 at.% Tb, T_{comp} of (a-1) lies below T_a while T_{comp} of (a-2) above T_a. Some distinct differences in the configuration of the recorded bits can be clearly noticed ; i.e.,

1) As the bias field strength(H_b) becomes smaller down from $H_b=+300$ Oe, bit domain size appears to remain unchanged in Fig.2 (a-1) even under negative bias field while in (a-2) it decreases gradually. Within the range of H_b applied in this work, (a-1) exhibit larger bit size than (a-2).

2) In film (a-1), the bit domains recorded at $H_b>0$ show uniform contrast, indicating that each bit is effectively single domain. The bit recorded at $H_b=0$, however, shows uneven domain contrast inside the bit, suggesting the presence of small subdomains with magnetic polarization antiparallel to that of the parent bit domain. As H_b increases negatively, area fraction of subdomains increases leaving only the rim of the bit at $H_b=-100$ Oe. At $H_b<-100$ Oe this film was not recordable. It can also be noted that domain contrast is decreasing as H_b increases negatively. Such features are never observed in (a-2) maintaining uniform and homogeneous contrast throughout the recordable range of H_b.

3) Film (a-1) produces uniform circular bits with smooth domain boundaries at all recordable H_b ranges while the domain shape of film (a-2) is irregular. The domain boundary of (a-2) is smooth at high H_b above 200 Oe but become increasingly rougher as H_b decreases.

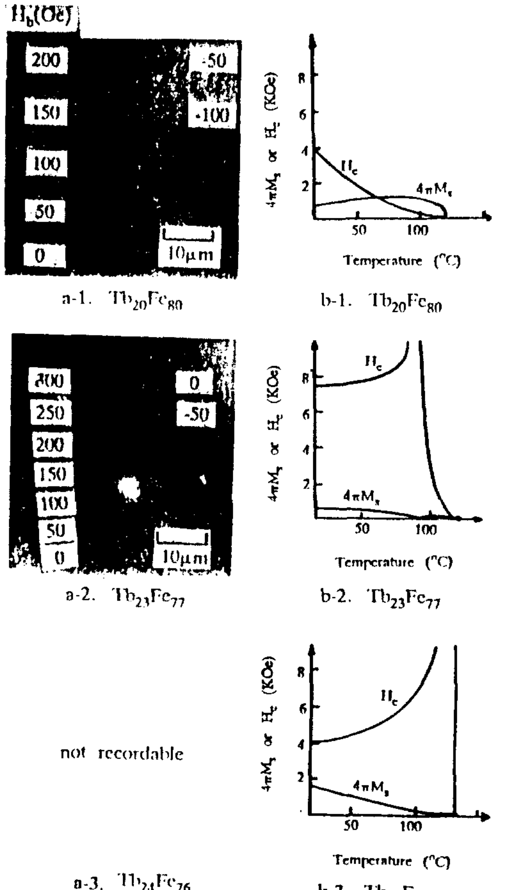

Fig.2 (a) Variation of bit size and shape under various bias fields. (b) [$4\pi M_s$ and H_c] vs. T for each film.

Clear distinction of recording characteristics between both types across the compensation composition is dramatically demonstrated in Fig.3 where the boundary between dark and light area in this film with compositional gradient delineates the line of compensation composition.

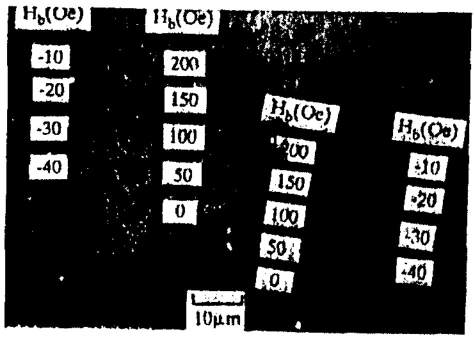

Fig.3 Variation of bit shape under various bias fields in TbFe film having compensation composition ($T_a = T_{comp}$)

For a given laser beam recording condition employed in this work the bit size decreases with increase of Tb content up to the compensation composition. Above the compensation composition bit size tends to increase with Tb content for a given H_b. Fig.4 summarizes the bit domain characteristics observed on TbFe film of a wide range of composition. It is interesting to note that the bit size become more sensitive to H_b as T_{comp} approaches T_c as this reflects the fact that the coercivity drop near T_c is increasingly steeper as T_{comp} approaches T_c. The H_b effect on the domain size is illustrated more clearly in Fig.5.

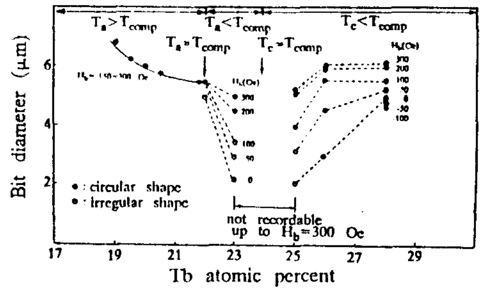

Fig.4 Variation of bit diameter recorded under various bias fields for different compositions of TbFe films.

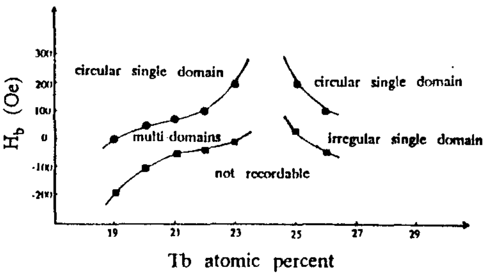

Fig.5 Domain shape variation of thermomagnetically written bits under various bias fields for different compositions of TbFe films.

3-3. Thermomagnetic Recording Characteristics of TbFeCo Films

A number of MO disks announced so far employs TbFeCo base media as the addition of Co in TbFe improves θ_k[5]. But since it accompanies enhancement of T_c as well as saturation magnetization(M_s) , the content of Co is usually limited in order to secure reasonable recording sensitivity and perpendicular magnetization of the active layer. Thermomagnetic recording test in our laboratory on TbFeCo films has shown a variety of domain configurations depending on the composition and the categorization of the recording characteristics as in the case of binary TbFe is not possible at present. Only the results for the films

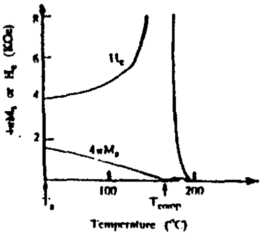

a-1. $Tb_{28}Fe_{59}Co_{13}$ b-1. $Tb_{28}Fe_{59}Co_{13}$

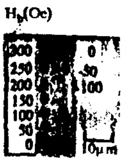

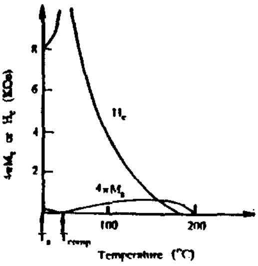

a-2. $Tb_{23.5}Fe_{65.5}Co_{11}$ b-2. $Tb_{23.5}Fe_{65.5}Co_{11}$

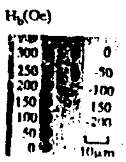

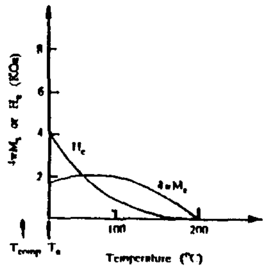

a-3. $Tb_{19.5}Fe_{71}Co_{9.5}$ b-3. $Tb_{19.5}Fe_{71}Co_{9.5}$

Fig.6 Domain shape variation of thermomagnetically written bits under various bias fields (a), and temperature dependence of H_c and $4\pi M_s$ (b) for different composition of TbFeCo films.

containing approximately 10 at.% Co and therefore having approximately the same T_c($\approx$ 200°C) are presented here since they exhibit recording characteristics corresponding to those of TbFe. Fig.6(a) show domain characteristics of 3 different TbFeCo films, namely (a-1),(a-2) and (a-3) with compositions $Tb_{28}Fe_{59}Co_{13}$, $Tb_{23.5}Fe_{65.5}Co_{11}$ and $Tb_{19.5}Fe_{71}Co_{9.5}$, respectively. The composition of each film may be categorized according to the case of TbFe as in Fig.4 ; i.e., (a-1) : $T_a << T_{comp} < T_c$, (a-2) : $T_{comp} > T_a$, (a-3) : $T_{comp} < T_a$. It can, however, be easily noticed that TbFeCo films do not appear to produce domains of the type corresponding to that for TbFe belonging to the same composition category. Rather, each domain characteristics of a-1, a-2 and a-3 is similar to those of type B, type A and type A, respectively. This implies that the recording characteristics of RE-TM films can not be predicted simply by the atomic species and composition unless the micromagnetical mechanisms of domain reversal in the course of laser heating and cooling is understood quantitatively.

4. Disucssion

4-1. Equilibrium Domain Size

Since the size, shape and micromagnetical domain structures of the recorded bit are determined by thermomagnetical response of the film to the spatial and temporal temperature change, it is essential to know the temperature dependence of magnetical parameters of the film which is relevant to the recording process. The stability criterion of a cylindrical bubble domain with radius r in a film of thickness h at any given temperature is given by [6]

$$-\frac{\sigma_w}{2r} - \frac{\partial\sigma_w}{2\partial r} + MH_d + MH_b \leq MH_c \qquad (1)$$

where σ_w is the wall energy, H_d is the demagnetizing energy and M is the magnetization at domain wall position.

Thus equilibrium domain size can be calculated if the values of σ_w ,M, H_d and H_c as functions of temperature are available. However, determination of wall energy and spatial distribution of H_d is practically difficult either experimentally or theoretically. If it can be assumed that the wall energy terms constitute H_c implicitly, Equation (1) can be simplified as

$$H_d + H_b \leq H_c \qquad (2)$$

For comparative evaluation of bit size between films with different magnetic properties, further approximation of H_d as $4\pi M_s$ may be justified reasonably, unless the size difference of the bits is excessively great, namely;

$$4\pi M_s(T_o) + H_b \leq H_c(T_o) \qquad (3)$$

The radius r_o from the beam center as illustrated in Fig.1 where T_o satisfies Equation (3) at any instance during the recording cycle may be regarded as the instantaneous domain radius. Final domain size at room temperature after a recording cycle will be equal to the largest r_o attained during the recording cycle since σ effect is ignored here. However, Shieh et al[7] examined domain formation process using high speed camera and observed that the domain size shrinks by 5-10% of the maximum upon cooling to room temperature. This implies that the position of domain wall formed at maximum T_o moves inward during cooling below T_o which must be driven by wall energy. Full account of the domain formation process may not be possible until wall energy and domain formation kinetics are clarified fully. But for the purpose of comparative examination of the present observations this also means that the arguments mentioned as above is reasonable enough since the evaluation of domain size can be accomplished according to Eq. (3) within 5-10% error range.

4-2. Temperature dependence of H_c and M_s

Fig.7 and 8 show temperature dependence of $4\pi M_s$ and H_c of various compositions, for TbFe and TbFeCo, respectively. Curves were constructed mostly with data taken from literatures[2,7] except those decorated with filled circles, the values measured in this work. It should be noted that the increase of Tb results in slight increase of T_c but steep increase of T_{comp}. As the temperature approaches toward T_c, the slope of H_c drop becomes increasingly greater as Tb content increases, within a few at.% range around compensation composition, while maximum value of M_s between T_{comp} and T_c decreases. Since TbFe has much lower T_c($\approx$ 130°C) than TbFeCo ($\approx$200°C within 10 at.% Co), the latter exhibits higher maximum M_s between T_{comp} and T_c than the former for a given Tb content, the difference being greater if T_c is raised further by adding more Co.

Origin of the differences in recording characteristics between the types described in 3-2 as well as between the alloy systems described in 3-3 may be revealed by comparing the [H_c and $4\pi M_s$] vs. T curves of each corresponding film, as presented in Fig.2(b) and 6(b), respectively. Since T_{peak} (=225°C) achieved at maximum heating during a recording cycle exceeds T_c's of both alloy systems, it may be reasonable to state that the recorded domain characteristics is mainly determined by the interaction between H_c and $4\pi M_s$ near T_c on cooling because H_c increases much more steeply than $4\pi M_s$ on further cooling below T_0. Comparison of the [H_c and $4\pi M_s$] vs. T curves near T_c of each film clearly reveals that those films producing type A domains commonly exhibit fairly high $4\pi M_s$ level and cross over with H_c-T curve on cooling below T_c(Fig.2 b-1. and Fig.6 b-2,3) whereas those belonging to type B have exceedingly small $4\pi M_s$ level in contrast to their steeply rising H_c so that H_c maintains higher level than $4\pi M_s$ below T_c (Fig.2 b-2. and Fig.6 b-1.). Films with $T_{comp}=T_c$ as in the case of Fig.2 b-3. will be unrecordable because H_c rises almost instantly when T drops just below T_c, whereas M_s maintains negligibly small values. It should be noted that the recording characteristics is dependent only on thermomagnetic properties of the film regardless of whatever atomic species constitute the film.

4-3. Domain Formation Mechanism

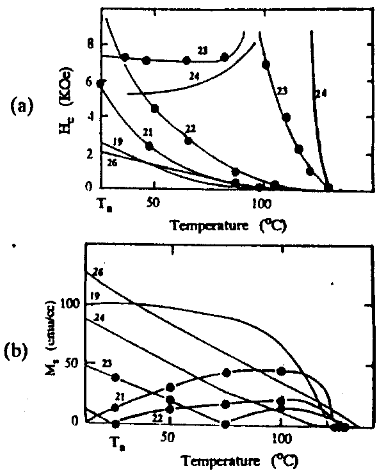

Fig.7 Temperature dependence of H_c and M_s for TbFe films of various compositions solid lines are taken from literature values [2,7] and dots are measured values in this work.

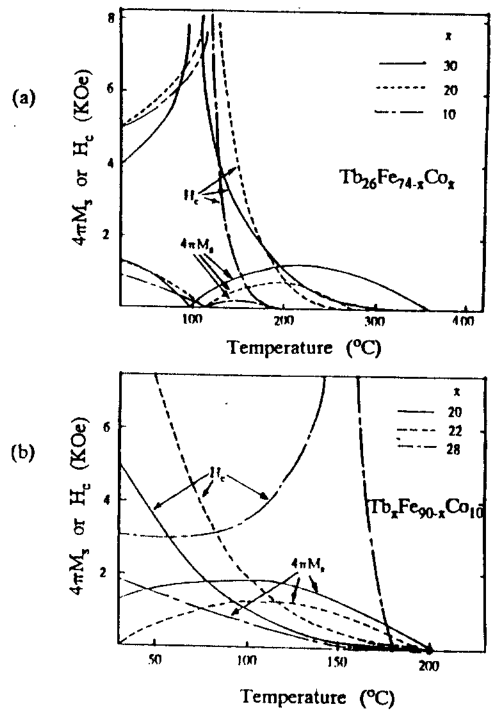

Fig.8 (a) Temperature dependence of H_c and $4\pi M_s$ of $Tb_{26}Fe_{74-x}Co_x$. (b) Temperature dependence of H_c and $4\pi M_s$ of $Tb_xFe_{90-x}Co_{10}$.

By combining the calculation of temporal temperature distribution in the film during the recording cycle with [H_c and $4\pi M_s$] vs. T curves it is possible to trace the micromagnetical domain formation process in a film. Fig.9 and 10 show schematic illustrations of spatial distribution of H_c and $4\pi M_s$ for typical type A and type B films, respectively, at several stages of cooling cycle. For type A as in Fig.9, $4\pi M_s$ exceeds H_c at the temperature between T_0 and T_c and exhibits a peak just near $r(T_0)$. This causes magnetization reversal due to the demagnetizing field H_d^1 in a narrow ring-shaped region of radius r_0(Fig.9-b). The radius of this ring-shaped region is largest at maximum heating. And this boundary remains as a domain wall which is frozen as soon as cooling. As T_{peak} approaches T_c on cooling, both $r(T_0)$ and $r(T_c)$ moves toward the beam center and broadening of the ring-shaped region occurs. The demagnetizing field H_d^2 (Fig.9-c) induced by magnetization of ring-shaped region produces another concentric ring-shaped domain of reverse polarization with respect to that of outer ring. This process will be repeated until $T_{peak} < T_0$ thus resulting in a bit filled with subdomains of concentric ring shape. Presence of positive (or negative) bias during the recording cycle has the effect to increase (or decrease) H_d^1. This H_b not only makes the domain saturated (or unsaturated) but also extends (or shrinks) $r(T_0)$.

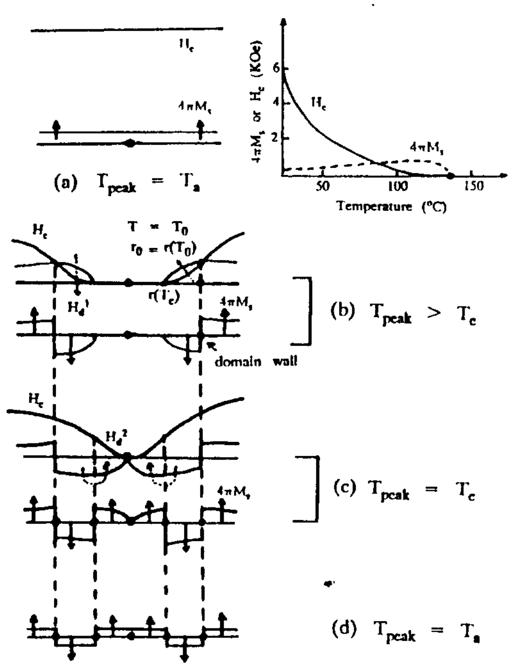

Fig.9 Schematic representation of domain reversal mechanism during thermomagnetic writing of TbFe films with composition of $T_a > T_{comp}$.

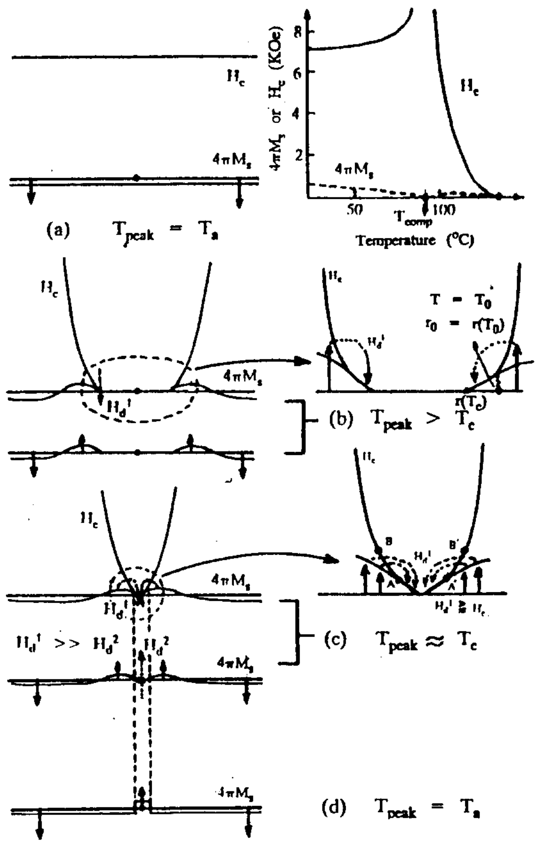

Fig.10 Schematic representation of domain reversal mechanism during thermomagnetic writing of TbFe films with composition of $T_a < T_{comp}$.

Hence, the bit size should be larger (or smaller) with increasing H_b, but this contradicts the experimental observation in type A films. Possible explanation for this discrepancy may be that the direction of magnetization of the film in the region between $r(T_0)$ and $r(T_c)$ deviates from the normal to the film plane by the external field, so that the normal component of M_s will be effectively reduced. Independence of bit size on the bias field observed in type A films may thus be due to fortuitous compromise between these two mutually opposite effects, at least in the range of H_b studied in this work. For higher H_b, however, domain size may change because the shape of [normal component of M_s] - T curve itself will be changed. Further work is certainly needed for clarification of detailed mechanism. Subdomain structure in a bit must also be influenced by the polarity and magnitude of H_b ; as H_b increases, H_b parallel to H_d^1 will extend the area of reverse polarization and finally forming a single domain , while H_b antiparallel to H_d^1 reduces it and finally leaving only the rim before complete disappearance. On the other hand, domain formation process of type B films is quite different in that $4\pi M_s$ never exceeds H_c substantially at any area of the film at $H_b=0$ and that change of magnetic polarization occurs across T_{comp} during cooling. Therefore H_d^1 just outside the circle of $r(T_c)$ is too weak to produce magnetization reversal at maximum heating. As T_{peak} approaches T_c on cooling $r(T_c)$ approaches zero(Fig.10-c) which results in concentration of H_d^1 on a tiny localized spot at the beam center. Domain reversal may occur depending on the configuration of $[H_c$ and $4\pi M_s]$ vs. T curve of the film as observed in Fig.2 (a-2). Domains in this case are likely to assume irregular shape since $r(T_o)$ will fluctuate sensitively even by a slight variation of the relative magnitude of H_d^1 and H_c near T_c because $H_d^1 \approx H_c$ between A and A', as shown in Fig.10-c. With increasing bias field $H_d^1+H_b$ curve will cross H_c at B and B' and thus the bit will grow in size and the domain boundary getting smoother.

4-4. Bit Size vs. Composition

Variation of bit size with composition as shown in Fig. 4 may be understood by following the argument of 4-1 since major parameter determining the bit size is found to be $r(T_o)$. Fig.11 compares values of T_o and $r(T_o)$ predicted by combining Fig.1 and 7 with measured size, for various TbFe films. For $H_b=0$ predictions matches reasonably well with the measurements, but for $H_b=300$ Oe considerable discrepancies exist particularly in type B films. This implies that the present model of domain formation process can be applied to the case of type A semi-quantitatively but not to the case of type B when H_b is involved.

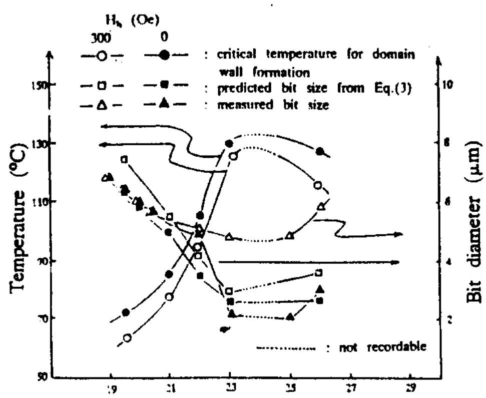

Fig.11 Relationship between bit size and critical temperature for domain wall formation after Eq.(3).

5. Conclusion

1) Thermomagentic recording characteristics of an amorphous TbFe and TbFeCo thin films is dependent critically on the relative magnitude of coercive force vs. demagnetizing field in the narrow range of temperature just below Curie temperature. Those having substantially higher $4\pi M_s$ than H_c near T_c produce circular bits and bit size is almost independent of bias field in the range of 300 Oe. These exhibiting only marginal difference between H_c and $4\pi M_s$ near T_c produces irregular bit shape at low bias field and bit size grows rapidly with increasing bias field. Those having T_{comp} located near T_c are unrecordable due to the excessively large H_c near T_c.

2) Micromagnetical mechanisms of the domain formation process need to be analyzed more precisely by incorporating the effect of domain wall energy and magnetization reversal kinetics so that they could be applied for other alloy systems not discussed yet in this work.

References

1. M.H. Kryder, J. Appl. Phys., 57, 3913 (1985)
2. S. Takayama, T. Niihara, K. Kaneko, Y. Sugita and M. Ojima, J. Appl. Phys., 61, 2610 (1987)
3. H.P. Shieh and M.H. Kryder, J. Appl. Phys., 61, 1108 (1987)
4. S.K. Lee and S.G. Kim, Adv. in Magneto-Optics, Proc. Int. Symp. Magneto-Optics, J. Magn. Soc. Jpn. Vol. 11, Suppl., No. S1, 317 (1987)
5. N. Imamura, S. Tanaka, F. Tanaka and Y. Nagao, IEEE Trans. Magn., MAG-21, 1607 (1985)
6. A.A. Thiele, Bell Sys. Tech. J., 48, 3287 (1969)
7. H.P Shieh, Ph.D. Thesis, Carnegie Mellon University (1987)